



HAL
open science

Effect of high hydrostatic pressure on the structure of the soluble protein fraction in *Porphyridium cruentum* extracts

Thierry Tran, Céline Lafarge, Rémi Pradelles, Jean-Marie Perrier-Cornet, Nathalie Cayot, Camille Loupiac

► To cite this version:

Thierry Tran, Céline Lafarge, Rémi Pradelles, Jean-Marie Perrier-Cornet, Nathalie Cayot, et al.. Effect of high hydrostatic pressure on the structure of the soluble protein fraction in *Porphyridium cruentum* extracts. *Innovative Food Science & Emerging Technologies / Innovative Food Science and Emerging Technologies*, 2019, 58, pp.102226. 10.1016/j.ifset.2019.102226 . hal-02321268

HAL Id: hal-02321268

<https://institut-agro-dijon.hal.science/hal-02321268>

Submitted on 20 Jul 2022

HAL is a multi-disciplinary open access archive for the deposit and dissemination of scientific research documents, whether they are published or not. The documents may come from teaching and research institutions in France or abroad, or from public or private research centers.

L'archive ouverte pluridisciplinaire **HAL**, est destinée au dépôt et à la diffusion de documents scientifiques de niveau recherche, publiés ou non, émanant des établissements d'enseignement et de recherche français ou étrangers, des laboratoires publics ou privés.



Distributed under a Creative Commons Attribution - NonCommercial 4.0 International License

1 **Effect of high hydrostatic pressure on the structure of the soluble protein**
2 **fraction in *Porphyridium cruentum* extracts.**

3

4 Thierry Tran¹, Céline Lafarge¹, Rémi Pradelles², Jean-Marie Perrier-Cornet^{1, 3}, Nathalie
5 Cayot¹, Camille Loupiac^{1 *1}

6 ¹ *Univ. Bourgogne Franche-Comté, AgroSup Dijon, PAM UMR A 02.102, F-21000 Dijon,*
7 *France*

8 ² *Microphyt, 713, route de Mudaison, 34670 Baillargues, France*

9 ³ *Dimacell Imaging Facility, AgroSup Dijon, CNRS, INRA, Univ. Bourgogne Franche-*
10 *Comté, F-21000 Dijon, France*

11

12

13 **Declaration of interest:** none

14

*1Corresponding author: Camille Loupiac, AgroSupDijon Esplanade Erasme 21000 Dijon, France. ph. +33 3 80
77 40 84 ; e-mail address: camille.loupiac@agrosupdijon.fr

Abbreviations: APC (allophycocyanin), B-PE (B-phycoerythrin), b-PE (b-phycoerythrin), HHP (high hydrostatic
pressure), Micro-DSC (micro-differential scanning calorimetry), PBR (photobioreactor), R-PC (R-phycoerythrin).

15 **Abstract**

16 High hydrostatic pressure (HHP) treatments are trending as “green” stabilization and
17 extraction process. The extraction of B-phycoerythrin from microalgae is getting more and
18 more interest due to its numerous potentialities in foods, cosmetics and medicine. Thus, the
19 effects of high pressure on the structural characteristics of B-phycoerythrin extracted from
20 *Porphyridium cruentum* are explored in this paper.

21 Spectrophotometric methods allowed to measure B-phycoerythrin content (UV-visible) and
22 gave an indication on the protein structure (fluorescence). Micro-DSC analysis and
23 electrophoresis complemented this structural investigation for all the protein fractions of
24 *P. cruentum* extracts.

25 Applying high hydrostatic pressure treatments up to 300 MPa during five minutes had no
26 significant effect on B-phycoerythrin content and structure in *P. cruentum* extracts.
27 Nevertheless, conformational changes of the protein are suggested by fluorescence yield
28 decrease at 400 MPa, and protein aggregation of B-phycoerythrin, observed by Micro-DSC
29 and electrophoresis, occurred at 500 MPa.

30

31 **Industrial relevance**

32 The HHP process is an emerging technology for the microbiological stability of various food
33 matrices, including the proteins of microalgae as natural colorant. The target pressure to
34 stabilize is around 400 MPa. High hydrostatic pressure can be used on *P. cruentum* extracts
35 up to 300 MPa without any change in protein structure, as the threshold of protein aggregation
36 is observed at 400 MPa. The observed changes of the proteins structure after applying HHP
37 above 400 MPa can have a strong impact at macroscopic scale on the food matrices: increase
38 of turbidity, change of texture, stability of emulsion.

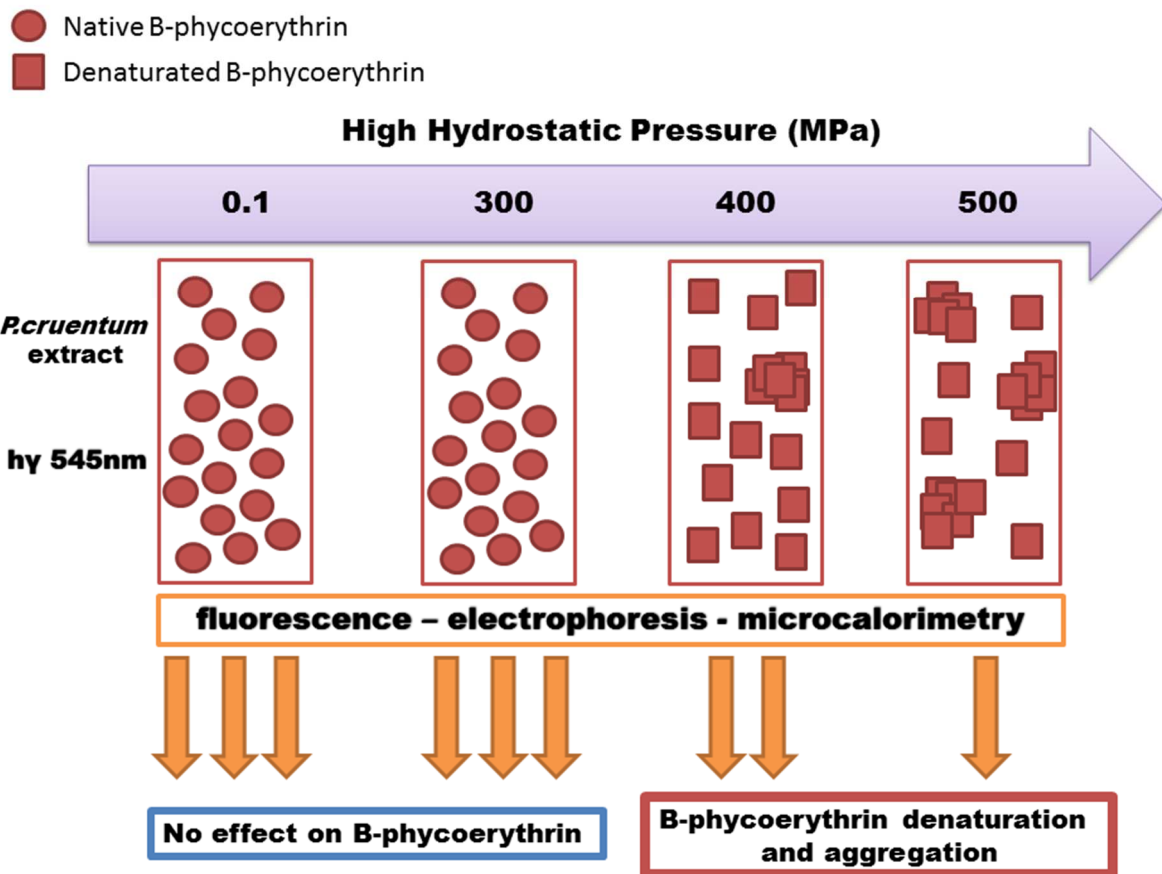
39

40 **Keywords**

41 High hydrostatic pressure, B-phycoerythrin, spectroscopy, structure, protein,
42 *Porphyridium cruentum*.

43

44 **Graphical abstract**



45

46

47 **Highlights:**

- 48 - A pressure of 400 MPa induced a change of conformation of the protein
- 49 - A treatment at 400 MPa induced the apparition of protein aggregates
- 50 - Protein structure was observed by fluorecence, electrophoresis, microcalorimetry
- 51 - B-phycoerythrin and b-phycoerythrin reached a stability limit at 300 MPa.

52 1. Introduction

53 *Porphyridium cruentum* is a spherical unicellular red alga (Rhodophyta) without any
54 organized cell wall (Jones, Speer, & Kury, 1963). This microalga is photoautotrophic and is
55 encapsulated in an exopolysaccharide sheath (Arad, Adda, & Cohen, 1985). Photosynthesis is
56 achieved by the lamella-shaped thylakoids that host the photosynthetic material (Gantt &
57 Conti, 1965).

58 *P. cruentum* hosts numerous pigment proteins, such as B-phycoerythrin (B-PE). This
59 macromolecule is part of a bigger protein structure called phycobilisome that involves other
60 proteins of the same family (phycobiliproteins) (Gantt & Lipschultz, 1972; Glazer, 1982).

61 *P. cruentum* phycobilisomes host three phycobiliproteins: allophycocyanin, phycocyanin and
62 phycoerythrin. Allophycocyanin acts as a core to which are attached the other proteins
63 arranged in rods. Those rods are composed of phycoerythrin in the extremity of the rods
64 attached to the core and phycocyanin is located between allophycocyanin and phycoerythrin
65 (Glazer, 1982). The amounts of phycobiliproteins of *P. cruentum* and their spectral properties
66 reported in the literature are shown in Table 1. These proteins have gained importance in
67 commercial applications in many industrial sectors (food, cosmetics, pharmaceuticals and
68 textile), as the demand of natural colorants is increasing. Because of their spectroscopic and
69 biological properties, phycobiliproteins are fluorescent probes widely used in clinical
70 diagnostics, flow cytometry and immunochemistry (Sekar & Chandramohan, 2008).

71

72 The important B-phycoerythrin content of *P. cruentum* makes this microalga an ideal raw
73 material for extraction and study of this pigment protein. In fact, commercial B-phycoerythrin
74 is mainly used as fluorescent biomarker in medical sciences due to its safety aspect for human
75 patients (Glazer, 1994; Manirafasha, Ndikubwimana, Zeng, Lu, & Jing, 2016). Consequently,
76 its natural fluorescence facilitates the investigation of the protein structure response to

77 environmental conditions. The three-dimensional structure of phycoerythrin from *P. cruentum*
78 has been determined (Camara-Artigas *et al.*, 2012; Ficner & Huber, 1993). All
79 phycobiliproteins consist of two dissimilar subunits, α and β , of 17 kDa to 19 kDa
80 respectively, depending on the species. These subunits are associated to form a heterodimeric
81 complex called the ($\alpha\beta$) monomer, and sometimes an additional γ -subunit, which has been
82 proposed to be located in the center of the hexamer formed by a trimer of the ($\alpha\beta$) monomer
83 acting as a linker protein. The presence of this γ -subunit is the main structural difference
84 between b-phycoerythrin and B-phycoerythrin. The chromophores (phycobilins) are open-
85 chain tetrapyrroles attached to thioether bonds to cysteine residues of the α and β subunits.
86 The spectral properties of bilins are determined not only by the chemical nature of the
87 prosthetic groups, but are also influenced by their nearby proteins.

88 B-phycoerythrin stability towards different parameters has been studied by Munier *et al.*
89 (2014) as unpurified in phosphate buffer resulting from a “crude extract” of *P. cruentum* and
90 by González-Ramírez *et al.* (2014) as purified in phosphate or potassium buffer. Both studies
91 concluded that B-phycoerythrin’s pH stability ranged between 4 and 10, making this pigment
92 interesting for food application. At extremely low pH, the color darkened from pink to purple
93 and tended to bleach at extremely high pH. The pH dependence of B-phycoerythrin has been
94 studied and explained at the conformation structural level by Camara-Artigas *et al.* (2012).
95 Studies also pointed its important sensitivity to direct light exposure with a significant
96 decrease in 545 nm absorbance after 4 h at 4°C from 33.57 $\mu\text{mol m}^{-2} \text{s}^{-1}$ light intensity
97 (González-Ramírez *et al.*, 2014; Munier *et al.*, 2014). Towards temperature, B-phycoerythrin
98 remained stable between 0 and 40°C (Munier *et al.*, 2014). A study performed by circular
99 dichroism on this protein revealed two irreversible structural transitions at 65°C and 85°C at
100 pH4, with the latter being absent at pH7 and pH10. It has also been shown in this study that
101 the melting temperature of the protein is 77.5°C \pm 0.5 (González-Ramírez *et al.*, 2014).

102

103 In this paper, we experimentally explored the properties of B-phycoerythrin under high
104 hydrostatic pressure (HHP). Indeed, in recent years, HHP have attracted attention to food
105 processing and preservation as an alternative to pasteurization (Baptista, Rocha, Cunha,
106 Saraiva, & Almeida, 2016; Gayán, Govers, & Aertsen, 2017; Perrier-Cornet, Tapin, Gaeta, &
107 Gervais, 2005). HHP is an efficient non-thermal physical method to cause modification in
108 protein secondary structure. The fluid used to transmit the pressure is usually water. The
109 advantages of HHP are reduced energy costs, a “green” process with no use of chemicals, and
110 the avoiding of temperature-induced denaturation of active substances (Huang, Hsu, Yang, &
111 Wang, 2013).

112 Only few studies have been performed on the stability of B-phycoerythrin under HHP. The
113 impact of high hydrostatic pressure up to 300 MPa on the absorbance spectrum of a
114 *P. cruentum* extract in phosphate buffer has been studied by Brody & Stelzig (1983). A shift
115 of phycocyanin absorbance peak from 620 nm to 634 nm was observed as well as a shift from
116 545 nm and 565 nm to 550 nm and 570 nm respectively for phycoerythrin absorbance peaks.
117 Additionally, they measured an absorbance increase at 550 nm at a rate of to $1.4 \cdot 10^{-1} \text{ MPa}^{-1}$
118 and at 570 nm at a rate of $0.61 \cdot 10^{-4} \text{ bar}^{-1}$. The main hypothesis of the authors of this study to
119 explain these changes in spectral properties as function of the high pressure is correlated to a
120 configurational changes in the pigment-protein complex.

121

122 Therefore, the aim of the present study was to investigate, by using multiscale tools, the
123 structural characteristics of B-phycoerythrin, in crude *P. cruentum* extracts treated by HHP
124 ranging from 0.1 MPa to 500 MPa.

125

126 **2. Materials and methods**

127 **2.1. Materials**

128 The marine Rhodophyta *Porphyridium cruentum* (1380-1C) was provided by the SAG
129 Culture Collection (Göttingen, Germany). The microalga was grown by Microphyt
130 (Baillargues, France) in 5,000 L photobioreactor (PBR) consisting in 1.2 km of glass tubes
131 with co-circulation of liquid medium and CO₂ enriched air (Patent No. WO2010109108 A1,
132 2010; Muller-Feuga *et al.*, 2012). The PBR was set under a greenhouse in order to control
133 temperature (between 22 and 28 °C) and the intensity of natural light using curtains. The pH
134 set point of 7.5 was automatically controlled by CO₂ injection and monitored by an inline
135 Fermprobe F-235 pH probe from Broadley James (Silsoe, United Kingdom). Air was injected
136 continuously at rate of 35 L min⁻¹. The culture medium used is a marine type medium,
137 corresponding to a modified Hemerick's medium (Stein-Taylor, 1973). This medium was
138 modified by addition of N and P up to 20 and 4 mmol L⁻¹ respectively. Cultivation was
139 conducted in semi-continuous conditions, thus maintaining the exponential growth phase
140 during 85 days. Cells were harvested by bowl centrifugation at 6000 rpm for 60 min at room
141 temperature (maximum reachable temperature of 35°C) using a KG 8006 from GEA (Oelde,
142 Germany) and concentrated at the rate of around 10-13% dry weight. The biomass was frozen
143 at - 20°C in polyethylene bags, heat sealed, and stored at -20°C. The biomass was then
144 dispatched in aliquots in airtight glass bottles at - 18°C away from light. The total number
145 freezing/thawing cycle is 2 with freezing at - 18°C and thawing at room temperature.

146

147 **2.2. Preparation of protein extracts**

148 *P. cruentum* biomass was resuspended in 0.5M Tris HCl buffer pH 7 (Sigma Aldrich, Saint
149 Louis, USA) at the rate of 3% (w/v) dry weight equivalent under magnetic stirring for one
150 hour at room temperature away from direct light exposure. The suspension was then
151 centrifuged (Sorvall RC6 (Thermofischer Scientific, Waltham, USA) with a SLC-3000 rotor)

152 at 5000g for 20 minutes at 20°C. The extract corresponds to the supernatant, the pellet was
153 discarded.

154

155 **2.3. Application of high hydrostatic pressure**

156 Homogenous samples of about 1.8 mL of *P. cruentum* extract were transferred to
157 polyethylene bags, which were then heat-sealed and placed in a high pressure vessel. They
158 were exposed to high pressures at 50, 100, 200, 300, 400 and 500 MPa at 20°C for 5 minutes
159 with a compression rate of approximately 1.6 MPa s⁻¹. The untreated sample was used as
160 control. The samples were made in triplicates for each pressure level.

161 The high-pressure treatments were performed in a high hydrostatic pressure vessel (Top
162 Industrie S.A., France). A hand operated pressure pump (Nowaswiss, Switzerland) was used
163 to obtain the pressure, using distilled water as pressure transmitting medium. A sheath Type K
164 thermocouple (Top Industrie S.A., France) was passed through the upper plug, and used to
165 measure and monitor the inner temperature of the vessel during the pressure treatment. The
166 sample chamber pressure was measured using a pressure gauge (SEDEME, France). This
167 system is the same as the one described and used in Perrier-Cornet *et al.* (2005).

168

169 **2.4. Characterization of proteins**

170 **2.4.1. Dry weight and protein content**

171 The dry weight ratio of *P. cruentum* extract was determined using gravimetric method: 10 g
172 of sample was kept 24 hours at 102°C in the oven and cooled down in a desiccator.

173 The total nitrogen determination was performed using elementary analysis with a Dumas
174 Nitrogen Analyzer NDA 701 (Velp Scientifica, Usmate, Italy). Dry samples were manually
175 ground. Then, a known weight of sample was inserted in a stainless-steel capsule for
176 mineralization by combustion. Total nitrogen content was converted to soluble protein content

177 using a nitrogen-to-protein ratio of 6.34 ± 0.04 , which was precisely determined for
178 *P. cruentum* extracts by Safi *et al.* (2013).

179 Three repetitions have been done by sample for the determination of dry weight and protein
180 content.

181

182 **2.4.2. UV- visible spectroscopy**

183 The suspension was then centrifuged (541/R with F45-30-11 rotor from Eppendorf
184 (Hambourg, Germany)) at 5000 g for 15 minutes at 4°C. The extract corresponds to the
185 supernatant, the pellet was discarded.

186 The absorbance spectrum between 220 and 800 nm was measured using a Monaco UVmc1
187 from Safas (Monaco) and semi-micro UV-cuvettes Brand (Wertheim, Germany). Extract
188 samples were diluted in Tris buffer 50 times to respect the Beer-Lambert law and each
189 modality was measured in triplicate.

190 The quantification of B-phycoerythrin in aqueous extracts was calculated using the following
191 equations firstly used by Bermejo, Alvarez-Pez, Acien Fernandez, & Molina Grima (2002):

192

$$193 \text{ [R-phycoyanin (R-PC)] (mg mL}^{-1}\text{)} = (\text{OD}_{620} - 0.7 \cdot \text{OD}_{650}) / 7.38 \quad (\text{Equation 1})$$

$$194 \text{ [Allophycocyanin (APC)] (mg mL}^{-1}\text{)} = (\text{OD}_{650} - 0.19 \cdot \text{OD}_{620}) / 5.65 \quad (\text{Equation 2})$$

$$195 \text{ [B-phycoerythrin] (mg mL}^{-1}\text{)} = (\text{OD}_{565} - 2.8 \cdot \text{[R-PC]} - 1.34 \cdot \text{[APC]}) / 12.7 \quad (\text{Equation 3})$$

196

197 OD₆₂₀, OD₆₅₀ and OD₅₆₅, correspond to the optical densities measured respectively at 620
198 nm, 650 nm and 565 nm. The B-phycoerythrin content was determined in mg mL⁻¹ and was
199 then converted in mg g⁻¹ dry biomass.

200 It is important to mention that this quantification method reflects the ability of the native
201 protein to emit at specific wavelengths and does not reflect the actual protein content.

202

203 **2.4.3. Fluorescence emission measurements**

204 Fluorescence emission spectra of B-phycoerythrin in *P. cruentum* extracts were measured
205 using a Fluorolog 3 T (Horiba, Kyoto, Japan). The excitation wavelength was 545 nm and
206 corresponded to the absorbance peak of B-phycoerythrin. Fluorescence emission was
207 measured between 555 and 700 nm with a step value of 0.5 and a slit of 1 nm. One
208 measurement was done per repetition, which is equivalent to 3 measurements per pressure
209 level.

210

211 **2.4.4. Electrophoresis in native conditions**

212 Invitrogen Novex Wedge Well 4-12% Tris-Glycine Gel (Thermo Fischer Scientific, Waltham,
213 USA) was used as migration gel with 0.3 % Tris pH 8.9 (CAS 77-86-1), 1.4 % glycine (CAS
214 56-40-6) buffer. Sample buffer was composed of 25 % glycerol (CAS 56-81-5), 12.5 % Tris
215 HCl 0.5M pH 6.8 and 0.05 % bromophenol blue (CAS 115-39-9). All reagents were
216 purchased at Sigma-Merck (Darmstadt, Germany). The NativeMark Unstained Protein
217 Standard Protocol molecular weight scale (Thermo Fischer Scientific, Waltham, USA) was
218 used at the rate of 10 μ L per well. 5 μ L of 50% extract and 50% sample buffer were
219 introduced in each well. 35mA was applied on a single gel. Revelation was performed
220 applying Coomassie blue (CAS 6104-58-1) and then the gel was rinsed with water.

221

222 **2.4.5. Electrophoresis gel image processing**

223 The electrophoresis gel was scanned by a Chemidoc MP device (BioRad, Hercules, USA) and
224 processes by the software Imagelab ver.5.1. (BioRad, Hercules, USA) with the following
225 parameters: 30 s exposure time, “Red epi” illumination and 695/55 filter. The relative band

226 intensity values were calculated relatively to the control sample (no HHP treatment
227 corresponds to 100%).

228

229 **2.4.6. Micro-differential scanning calorimetry (Micro-DSC)**

230 A precise amount of extract of about 500 mg was introduced in a micro-DSC device Setaram
231 MicroDSC III (Caluire-et-Cuire, France) with linear temperature profile of 0.5 K minute⁻¹
232 from 25 °C to 100 °C. The data treatment software associated with the device and used for the
233 peak integration is SETSOFT2000 v.1.2.

234 The parameters measured on the thermograms are: peak temperature (T_p), peak onset (T_{on})
235 and peak offset (T_{off}) temperatures and peak enthalpy (through integration). One measurement
236 was done per repetition, which is equivalent to 3 measurements per pressure level.

237

238 **2.5. Statistical analysis**

239 The statistical analysis of Micro-DSC data, principal component analysis (PCA) and
240 hierarchic cluster analysis (HCA) were performed using the software Statistica v.8. by
241 StatSoft, Inc (Paris, France). The statistical analysis of other data was processed by XLStat
242 v.14.0. by Addinsoft (Paris, France). Regardless of the software used, analysis of variance
243 (ANOVA) and confidence intervals were performed to determine significant differences
244 between the samples for a given parameter. Significance was established at $p < 0.05$. ANOVA
245 showing significant differences lead to the use of Newman-Keuls pair test.

246

247 **3. Results and discussion**

248 **3.1. Characterization of soluble protein extract**

249 The crude *P. cruentum* extract was characterized by a pH value of 7.23 ± 0.10 and a dry
250 weight of 8.25 ± 0.02 %. The nitrogen content of this dry weight was 7.49 % corresponding to

251 a protein content of 158.6 mg g^{-1} dry weight using the nitrogen-to-protein conversion factor of
252 6.34.

253 The spectrum between 220 nm and 800 nm of the extract (Figure 1-A) showed a characteristic
254 profile described for the first time by Gantt & Lipschultz (1974). Beside the 280 nm peak
255 corresponding to UV-absorbing substances such as protein, the other peaks are typical
256 markers of phycobiliproteins: the double peak at 545 nm and 565 nm along with the smaller
257 peak at 320 nm are related to B-phycoerythrin, whereas the peak around 620 nm and the
258 hardly distinguishable peak at 650 nm are linked respectively to R-phycoerythrin and
259 allophycoerythrin. The spectrophotometric measurements allowed the calculation of B-
260 phycoerythrin content of $66.11 \pm 0.69 \text{ mg g}^{-1}$ dry biomass and a purity index of 2.56 ± 0.04 .

261 In order to investigate specifically the structure of B-phycoerythrin, the extract was submitted
262 to an excitation wavelength of 545 nm, the fluorescence emission of B-phycoerythrin could
263 be measured (Figure 1-B). This fluorescence emission spectrum was close to the one observed
264 by Gantt & Lipschultz (1974) with a peak around 575 nm.

265
266 The molecular weight of the different protein fractions of the crude extract was determined by
267 electrophoresis in native conditions (Figure 2). In the control sample (well 1), several bands
268 were visible before coloration: an originally blue band above 480 kDa, two originally pink
269 intense bands around 242 kDa and a group of three originally pink bands ranging from less
270 than 66 kDa to 146 kDa. The same electrophoretic profile has been described by Gantt and
271 Lipschultz (1974). The pink bands were easily linked to B-phycoerythrin with the two intense
272 bands around 242 kDa being identified as charge isomers of B-phycoerythrin and the group of
273 bands of lower molecular weight representing the polydispersed forms of b-phycoerythrin
274 (meaning dimers and tetramers). It is worth to mention that the main difference between B-
275 phycoerythrin and b-phycoerythrin is the presence of a γ subunit of *ca.* 35 kDa in the B form,

276 which explains its high molecular weight (Glazer & Hixson, 1977). The blue band can be
277 linked to R-phycoyanin and this has been confirmed by spectrophotometry (Gantt &
278 Lipschultz, 1974). However, there is no explanation of why the R-phycoyanin band was
279 present above 480 kDa whereas its molecular weight has been determined between 103 kDa
280 and 125 kDa (Gantt & Lipschultz, 1974; Glazer & Hixson, 1975). A similar observation was
281 made by (Ma, Wang, Sun, & Zeng, 2003) involving R-phycoyanin and B-phycoerythrin
282 without making further comment. R-phycoyanin's position in native condition
283 electrophoresis should result from a higher aggregation state. As a matter of fact, R-
284 phycoyanin is known to assemble itself in hexamers under specific conditions (Glazer,
285 1982), although the hexamer association is not enough to explain the molecular weight above
286 480 kDa.

287

288 Complementary to electrophoresis, micro-DSC measurements were carried out to investigate
289 the thermodynamic behavior of the proteins in the extract. The thermogram of the control
290 sample is presented in Figure 3. It reveals two main endothermic peaks. These peaks can be
291 integrated to determine unfolding temperature and enthalpy of this unfolding process. For the
292 control sample, we observed a first peak (peak 1) at $58.8 \text{ }^\circ\text{C} \pm 0.9$ ($T_{\text{on}} = 53.8 \pm 2.8 \text{ }^\circ\text{C}$; $T_{\text{off}} =$
293 $64.3 \pm 1.2 \text{ }^\circ\text{C}$) with an enthalpy of $0,0433 \pm 0,0155 \text{ J g}^{-1}$ fresh sample, and a second peak
294 (peak 2) at $85.8 \text{ }^\circ\text{C} \pm 0.5$ ($T_{\text{on}} = 83.7 \pm 1.5 \text{ }^\circ\text{C}$; $T_{\text{off}} = 87.7 \pm 0.7 \text{ }^\circ\text{C}$) with an enthalpy of
295 $0,0141 \pm 0,0028 \text{ J g}^{-1}$ fresh sample. A third minor peak could be considered at $90.2 \text{ }^\circ\text{C} \pm 1.3$
296 ($T_{\text{on}} = 89.3 \pm 1.1 \text{ }^\circ\text{C}$; $T_{\text{off}} = 91.4 \pm 1.0 \text{ }^\circ\text{C}$) with an enthalpy of $0.0021 \pm 0.0016 \text{ J g}^{-1}$ fresh
297 sample. These results are reminiscent of the two main irreversible structural transitions at 65
298 $^\circ\text{C}$ and 85 $^\circ\text{C}$ revealed by González-Ramírez *et al.*, (2014) using circular dichroism with the
299 two first endothermic peaks appearing at similar temperatures.

300

301 **3.2. Effect of HHP on the soluble protein extract**

302 The spectral properties of the *P. cruentum* extract treated by high hydrostatic pressure were
303 measured to determine the evolution of B-phycoerythrin concentration and its fluorescence
304 emission yield (Table 2).

305 The B-phycoerythrin concentration remained stable between 0.1 and 400 MPa treatment but
306 underwent a significant loss ($p = 0.007$) at 500 MPa of *ca.* 4 mg g^{-1} dry biomass (6%)
307 compared to the untreated extract. The fluorescence yield of B-phycoerythrin also remained
308 stable between 0.1 and 300 MPa but showed a significant loss at 400 MPa (- 6 % compared to
309 control) that significantly increased at 500 MPa (- 20 % compared to control) ($p < 0.001$).
310 Those impacts on fluorescence properties of B-phycoerythrin suggest that high pressure
311 induced a conformation change of the protein from 400 MPa leading to its denaturation hence
312 the concentration decrease at 500 MPa.

313 The observation of the electrophoresis in native conditions (Figure 2) showed that increasing
314 high hydrostatic pressure treatment up to 300 MPa (wells 2 to 5) did not impact the
315 electrophoretic profile. The 400 MPa treatment (well 6) induced the apparition of protein
316 aggregates located at the bottom of the well originally wielding a pink color. Additionally, the
317 b-phycoerythrin bands of lower molecular weight tended to decrease (value intensity of 98,
318 Figure 2). With a 500 MPa treatment (well 7), the pink aggregates gained intensity and the B-
319 and b-phycoerythrin bands appeared even weaker (respectively, value intensity of 65 and 94,
320 Figure 2). This result suggests that B-phycoerythrin is more sensitive to pressure than b-
321 phycoerythrin between 400 MPa and 500 MPa. Moreover, the bands intensity **suggests**
322 opposite evolutions between the two forms with an increase of b-PE (value intensity from 97
323 to 108) and a decrease of B-PE band intensity (value intensity from 98 to 91) between 100
324 MPa and 300 MPa. The R-phycoerythrin band is heavily faded at 500 MPa (if not completely
325 absent) (Table 2).

326 These observations support the hypothesis that B-phycoerythrin and b-phycoerythrin reach a
327 stability limit towards pressure from 400 MPa with a clear loss at 500 MPa by undergoing
328 aggregation. This statement can be extended to R-phycoerythrin at 500 MPa. The
329 disappearance of bands could be related to the low initial concentration rather than intrinsic
330 resistance to pressure. Therefore, it is not possible to conclude that R-phycoerythrin showed
331 higher sensitivity to pressure than B- or b-phycoerythrin because of the limit of sensitivity of
332 the used methods.

333 Moving forwards to the impact of the effects of HHP, the micro-DSC data show no
334 significant evolution of the peaks' summit, onset, offset, width nor enthalpy, except for peak 2
335 with a significant decrease in enthalpy at 500 MPa ($p = 0.001$). This suggests a potential link
336 between peak 2 and B-phycoerythrin or R-phycoerythrin.

337 As a way to sum up the effects induced by HHP treatment on B-phycoerythrin in *P. cruentum*
338 extracts, a Principle Component Analysis (PCA) was performed (Figure 4). F1 is the main
339 axis with 85.80 % proper value and F2 only having 9.66 %. As expected, samples are strongly
340 distributed along the F1 axis with increasing pressure level from left to right (Figure 4-A).

341 The parameters are strongly correlated with the F1 axis: pressure and peak 3 enthalpy
342 positively and B-PE content, fluorescence yield, peak 1 enthalpy and peak 2 enthalpy
343 negatively. Increasing pressure levels in HHP treatments negatively impact the B-
344 phycoerythrin content and its fluorescence yield. The PCA also highlights the high correlation
345 between peak 2 and B-PE fluorescence yield (correlation value of 0.96, Table 3) which could
346 strongly suggest that peak 2 is related to the structure of B-phycoerythrin. Peak 1 enthalpy is
347 strongly negatively correlated to pressure (- 0.98, Table 3) which may tie this parameter to
348 native proteins, but not specifically B-phycoerythrin (correlation with B-PE content of 0.77
349 and with B-PE fluorescence yield of 0.70, Table 3). The groups formed according to
350 hierarchic cluster analysis (Figure 4-B) separates the 500 MPa treatment from control, 300

351 and 400 MPa treatments, indicating that the effects induced by HHP clearly happen at 500
352 MPa. Nevertheless, the 400 MPa treatment constitutes a sub-group alone and differentiates
353 itself from the control, confirming that modifications occurred from 400 MPa. The value of
354 this threshold 400 MPa is in agreement with the previous study performed by (Brody &
355 Stelzig, 1983) on *P. cruentum* and microalgae extract. Even if there is a lack of information in
356 the literature concerning the effect of HHP treatment on proteins in food matrices, and on the
357 mechanism of proteins unfolding under high pressure in presence of other ingredients, it is
358 now well establish that a pressure between 400 and 600 MPa inactivates most of the food
359 pathogens (Baptista *et al.*, 2016).

360

361 4. Conclusion

362 The HHP process is an emerging technology for the microbiological stability of various food
363 matrices, including the proteins of microalgae as natural colorant. The target pressure to
364 stabilize the food product is above 400 MPa. The results of our study show that the structure
365 of the proteins can be impacted at this level of HHP leading to aggregation at higher pressure.
366 In fact, five minutes HHP treatments up to 300 MPa had no significant effect either on B-
367 phycoerythrin content and structure in *P. cruentum* extracts. Nevertheless, signs of
368 conformational changes of the protein are suggested by fluorescence yield decrease from 400
369 MPa. This phenomenon might lead to protein aggregation of B-phycoerythrin occurring at
370 500 MPa. R-phycoerythrin content was also clearly impacted at 500 MPa and might undergo
371 the same denaturation path.

372 Previous studies aimed at characterizing model or isolated proteins under high pressure or
373 after applying high pressure. In the present study, the investigation was done on a protein
374 extract from microalgae with a mixture of proteins, and at a concentration relative of their
375 future use as colorant in food or cosmetic applications.

376 Indeed, with this complex matrix, we observed the structural change with different methods
377 (fluorescence, microcalorimetry, electrophoresis), which allows observing different levels of
378 structure. It is now well established that protein functionalities are linked to their structure.
379 The observed changes of the proteins structure after applying HHP can thus have a strong
380 impact at macroscopic scale on the food matrices: increase of turbidity, change of texture,
381 stability of emulsion. For example, in the case of the use of microalgae soluble extracts as
382 natural colorant in food or cosmetic matrices (such as drinks or emulsions), if high pressure
383 process is used as an emerging technology to avoid any microbiological contamination, the
384 molecular aggregation of the natural colorants which can happen at around 400 MPa can be
385 the cause of other changes in interaction with the other food ingredients.

386 At molecular scale, further studies are needed to improve the understanding of the behavior of
387 a mixture of proteins during high pressure processing and if possible at higher concentrations.

388

389 **Acknowledgements**

390 We thank Bernadette Rollin for her technical support.

391 The micro-DSC analysis was performed with equipment from technical platform “DIVVA”
392 (Développement Innovation Vigne Vin Aliments), AgroSup Dijon – Université de Bourgogne
393 Franche-Comté.

394 **Funding**

395 This work was supported by Conseil Régional de Bourgogne Franche Comté (PARI) and had
396 no specific role in the conduct of the research or in the writing of this paper.

397

398 **References:**

399 Arad, S. M., Adda, M., & Cohen, E. (1985). The potential of production of sulfated
400 polysaccharides from *Porphyridium*. *Plant and Soil*, 89(1–3), 117–127.

401 Baptista, I., Rocha, S. M., Cunha, Â., Saraiva, J. A., & Almeida, A. (2016). Inactivation of
402 *Staphylococcus aureus* by high pressure processing: An overview. *Innovative Food*
403 *Science & Emerging Technologies*, 36, 128–149.

404 Bermejo, R., Alvarez-Pez, J. M., Acien Fernandez, F. G., & Molina Grima, E. (2002).
405 Recovery of pure B-phycoerythrin from the microalga *Porphyridium cruentum*.
406 *Journal of Biotechnology*, pp. 73–85.

407 Brody, S. S., & Stelzig, L. (1983). Effect of pressure on the absorption spectra of
408 phycobiliprotein and *Porphyridium cruentum*. *Zeitschrift Für Naturforschung. Section*
409 *c, Biosciences*, 38c, 458–460.

410 Camara-Artigas, A., Bacarizo, J., Andujar-Sanchez, M., Ortiz-Salmeron, E., Mesa-Valle, C.,
411 Cuadri, C., Allen, J. P. (2012). pH-dependent structural conformations of B-
412 phycoerythrin from *Porphyridium cruentum*. *FEBS Journal*, 279(19), 3680–3691.

413 Ficner, R., & Huber, R. (1993). Refined crystal structure of phycoerythrin from *Porphyridium*
414 *cruentum* at 0.23-nm resolution and localization of the gamma subunit. *European*
415 *Journal of Biochemistry*, 218(1), 103–106.

416 Fuentes, M. R., Fernández, G. A., Pérez, J. S., & Guerrero, J. G. (2000). Biomass nutrient
417 profiles of the microalga *Porphyridium cruentum*. *Food Chemistry*, 70(3), 345–353.

418 Gantt, E., & Conti, S. F. (1965). The ultrastructure of *Porphyridium cruentum*. *The Journal of*
419 *Cell Biology*, 26(2), 365–381.

420 Gantt, E., & Lipschultz, C. A. (1972). Phycobilisomes of *Porphyridium cruentum*: I. Isolation
421 . *The Journal of Cell Biology*, 54, 313–324.

422 Gantt, E., & Lipschultz, C. A. (1974). Phycobilisomes of *Porphyridium cruentum*. Pigment
423 analysis. *Biochemistry*, 13(14), 2960–2966.

424 Gayán, E., Govers, S. K., & Aertsen, A. (2017). Impact of high hydrostatic pressure on
425 bacterial proteostasis. *Biophysical Chemistry*.

426 Glazer, A. N. (1982). Phycobilisomes: structure and dynamics. *Annual Reviews in*
427 *Microbiology*, 36(1), 173–198.

428 Glazer, A. N. (1994). Phycobiliproteins—a family of valuable, widely used fluorophores.
429 *Journal of Applied Phycology*, 6(2), 105–112.

430 Glazer, A. N., & Hixson, C. S. (1977). Subunit structure and chromophore composition of
431 rhodophytan phycoerythrins. *Porphyridium cruentum* B-phycoerythrin and b-
432 phycoerythrin. *Journal of Biological Chemistry*, 252(1), 32–42.

433 Glazer, A. N., & Hixson, C. S. (1975). Characterization of R-phycoyanin. Chromophore
434 content of R-phycoyanin and C-phycoerythrin. *Journal of Biological Chemistry*,
435 250(14), 5487–5495.

436 González-Ramírez, E., Andújar-Sánchez, M., Ortiz-Salmerón, E., Bacarizo, J., Cuadri, C.,
437 Mazuca-Sobczuk, T., Martínez-Rodríguez, S. (2014). Thermal and pH Stability of
438 the B-Phycoerythrin from the Red Algae *Porphyridium cruentum*. *Food Biophysics*,
439 9(2), 184–192.

440 Huang, H.-W., Hsu, C.-P., Yang, B. B., & Wang, C.-Y. (2013). Advances in the extraction of
441 natural ingredients by high pressure extraction technology. *Trends in Food Science &*
442 *Technology*, 33(1), 54–62.

443 Jones, R. F., Speer, H. L., & Kury, W. (1963). Studies on the growth of the red alga
444 *Porphyridium cruentum*. *Physiologia Plantarum*, 16(3), 636–643.

445 Ma, S.-Y., Wang, G.-C., Sun, H.-B., & Zeng, C.-K. (2003). Characterization of the artificially
446 covalent conjugate of B-phycoerythrin and R-phycoyanin and the phycobilisome
447 from *Porphyridium cruentum*. *Plant Science*, 164(2), 253–257.

448 Manirafasha, E., Ndikubwimana, T., Zeng, X., Lu, Y., & Jing, K. (2016). Phycobiliprotein:
449 Potential microalgae derived pharmaceutical and biological reagent. *Biochemical*
450 *Engineering Journal*, 109, 282–296.

451 Muller-Feuga, A. (2010). *Patent No. WO2010109108 A1*.

452 Muller-Feuga, A., Lemar, M., Vermel, E., Pradelles, R., Rimbaud, L., & Valiorgue, P. (2012).

453 Appraisal of a horizontal two-phase flow photobioreactor for industrial production of

454 delicate microalgae species. *Journal of Applied Phycology*, 24(3), 349–355.

455 Munier, M., Jubeau, S., Wijaya, A., Morançais, M., Dumay, J., Marchal, L., Fleurence, J.

456 (2014). Physicochemical factors affecting the stability of two pigments: R-

457 phycoerythrin of *Grateloupia turuturu* and B-phycoerythrin of *Porphyridium*

458 *cruentum*. *Food Chemistry*, 150, 400–407.

459 Perrier-Cornet, J.-M., Tapin, S., Gaeta, S., & Gervais, P. (2005). High-pressure inactivation of

460 *Saccharomyces cerevisiae* and *Lactobacillus plantarum* at subzero temperatures.

461 *Journal of Biotechnology*, 115(4), 405–412.

462 Safi, C., Charton, M., Pignolet, O., Silvestre, F., Vaca-Garcia, C., & Pontalier, P.-Y. (2013).

463 Influence of microalgae cell wall characteristics on protein extractability and

464 determination of nitrogen-to-protein conversion factors. *Journal of Applied*

465 *Phycology*, 25(2), 523–529.

466 Sekar, S., & Chandramohan, M. (2008). Phycobiliproteins as a commodity: trends in applied

467 research, patents and commercialization. *Journal of Applied Phycology*, 20, 113–136.

468 Stein-Taylor, J. R. (Ed.). (1973). *Handbook of phycological methods*. Cambridge: University

469 Press.

470

471 **Figure captions**

472

473 **Figure 1. (A) Normalized absorbance spectrum and (B) fluorescence emission spectrum**
474 **(545 nm excitation) of reference extract obtained from *Porphyridium cruentum* biomass**
475 **in 500mM pH 7 Tris buffer.**

476

477 **Figure 2. Migration of extracts obtained from *Porphyridium cruentum* biomass on**
478 **electrophoresis gels in native conditions at 4-12% of acrylamide. From left to right: well**
479 **1: 0 bar treatment (control); well 2: 50 MPa treatment; well 3: 100 MPa treatment; well**
480 **4: 200 MPa treatment; well 5: 300 MPa treatment; well 6: 400 MPa treatment; well 7:**
481 **500 MPa treatment; well 8: molecular weight scale (from top to bottom): 1236 kDa, 1048**
482 **kDa, 720 kDa, 480 kDa, 242 kDa, 146 kDa, 66 kDa, 20 kDa.**

483 **Numbers in white indicate the relative band intensity value (in %) obtained by image**
484 **processing.**

485

486 **Figure 3. Micro-DSC thermogram of reference extract obtained from *Porphyridium***
487 ***cruentum* biomass in 500mM pH 7 Tris buffer (control sample before HHP treatment).**

488

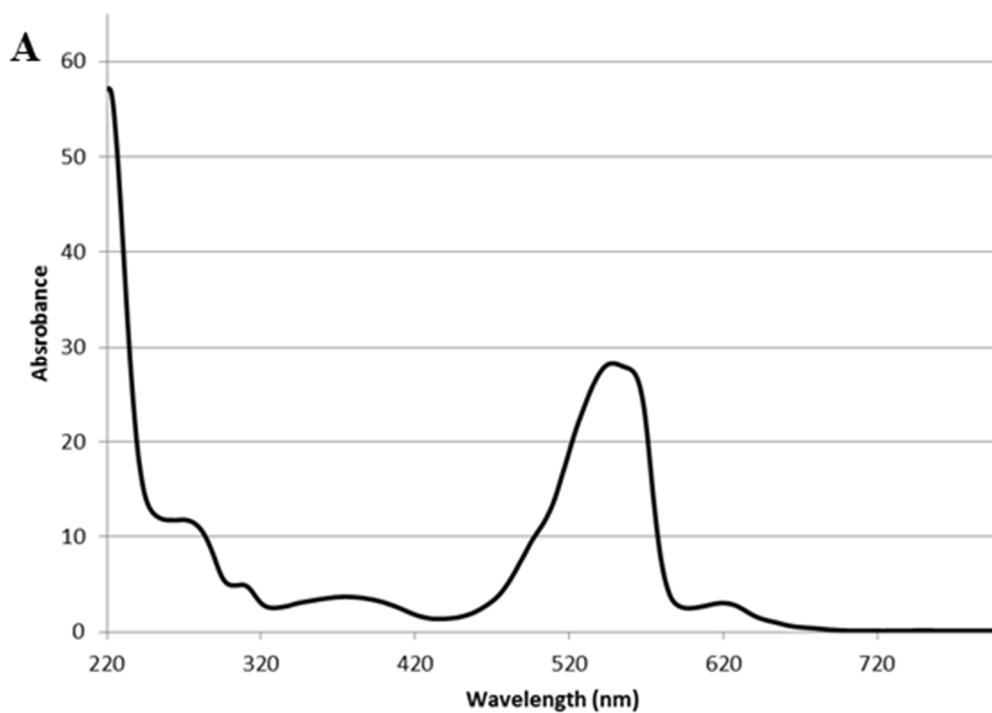
489 **Figure 4. (A) Results of PCA loading and (B) score plot of the different samples treated**
490 **at different HHP levels.**

491 **[B-PE] = B-phycoerythrin content.**

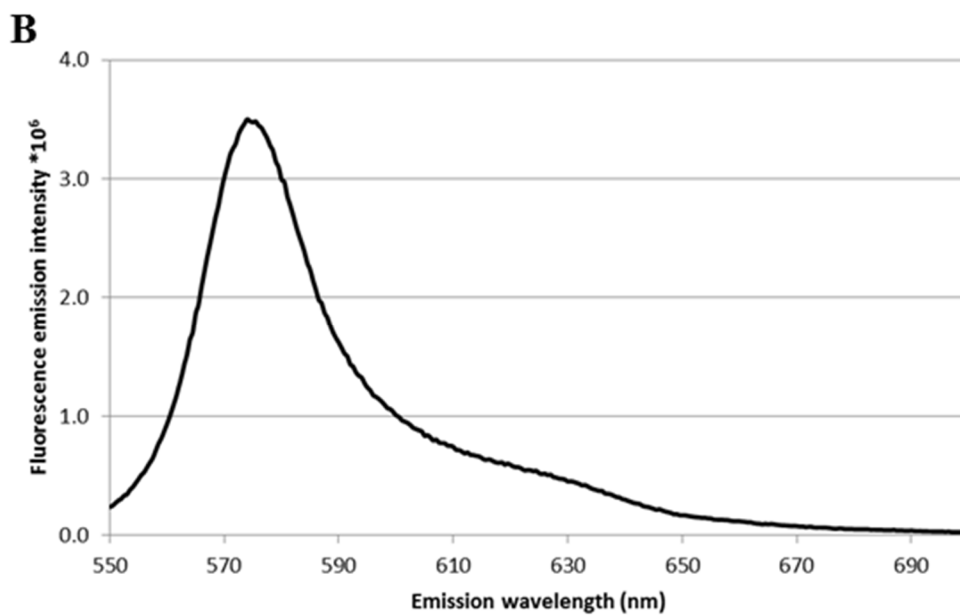
492 **Circles represent sample groups according to hierarchical cluster analysis.**

493

494 **Figure 1**



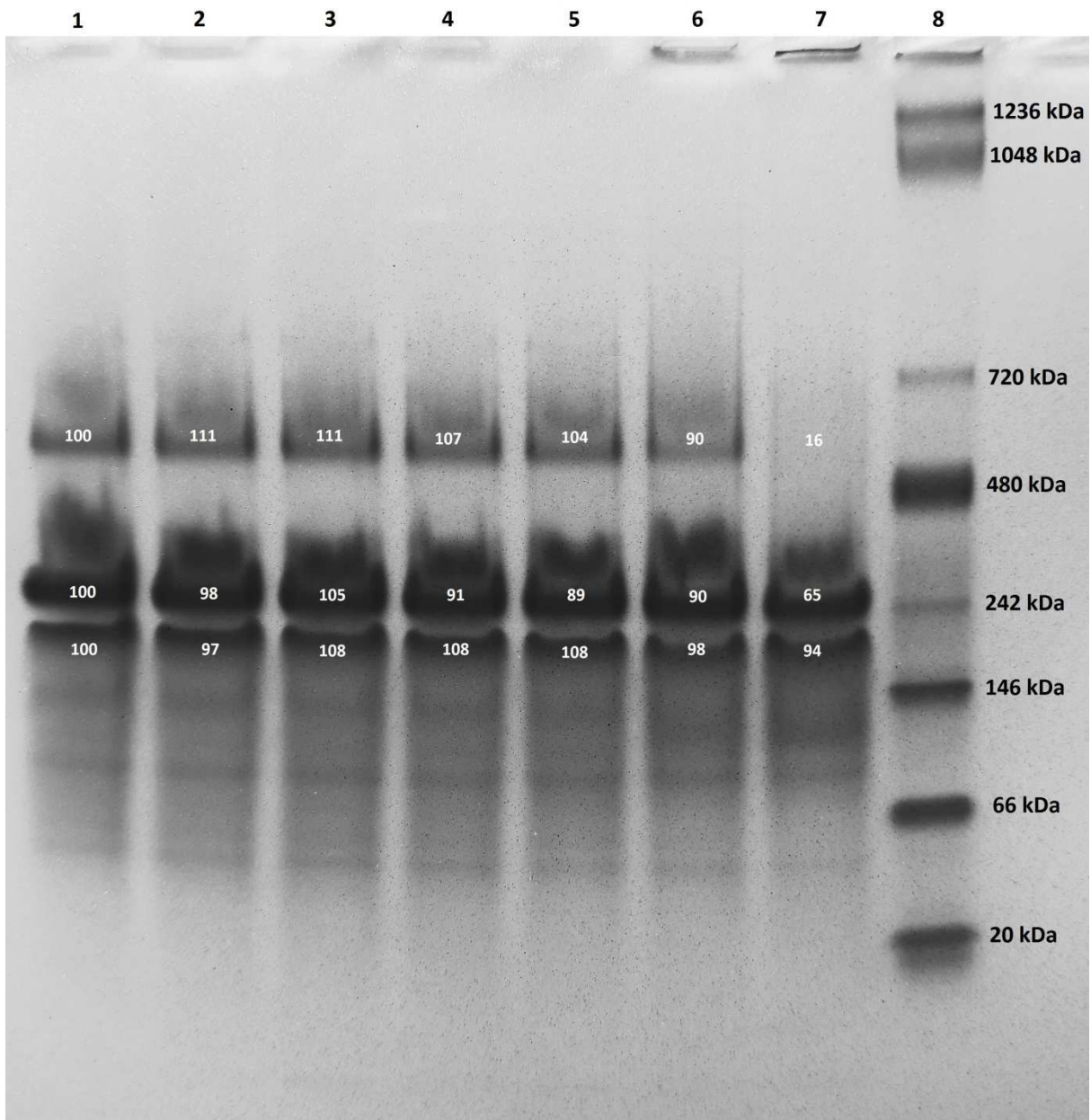
495



496

497

498 **Figure 2**



499

500

501

502

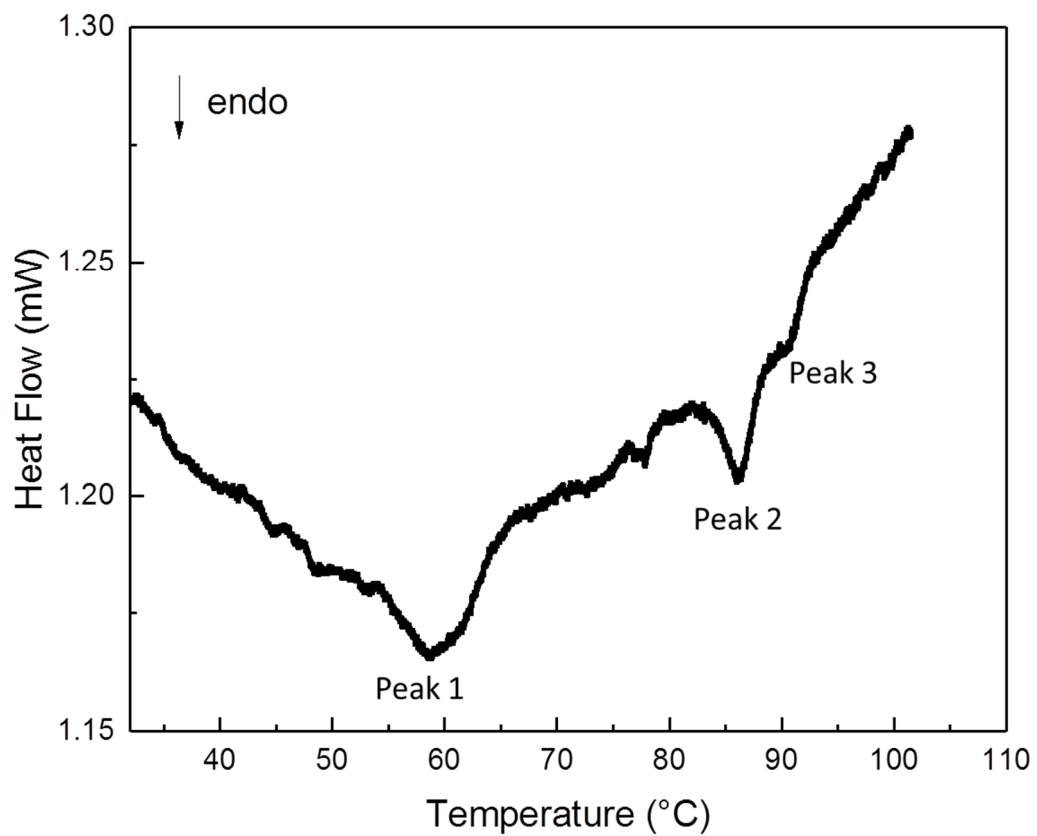
503

504

505

506

507 **Figure 3**



508

509

510

511

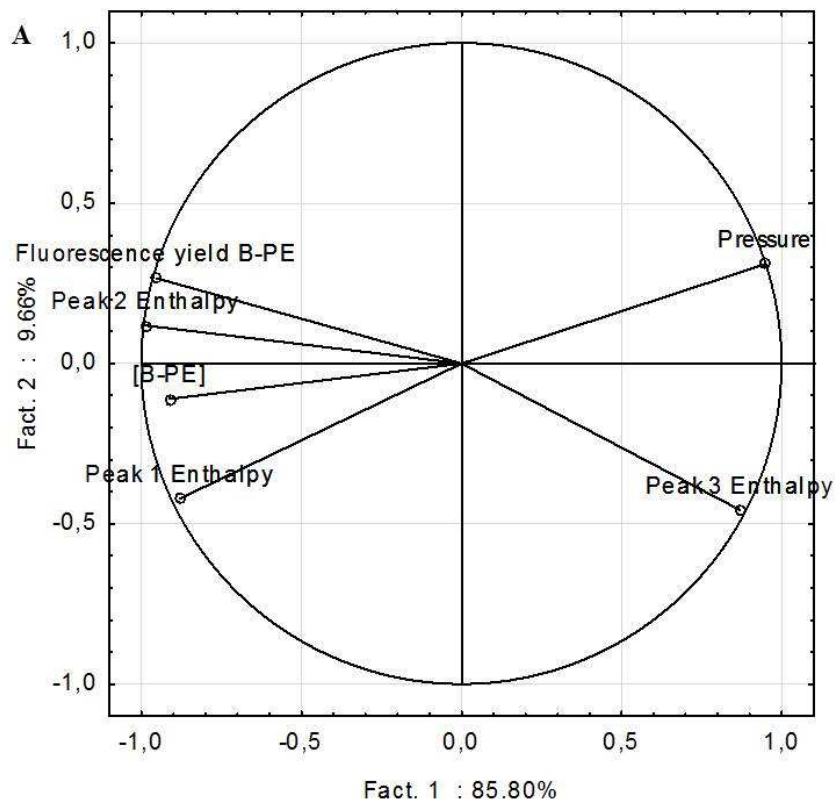
512

513

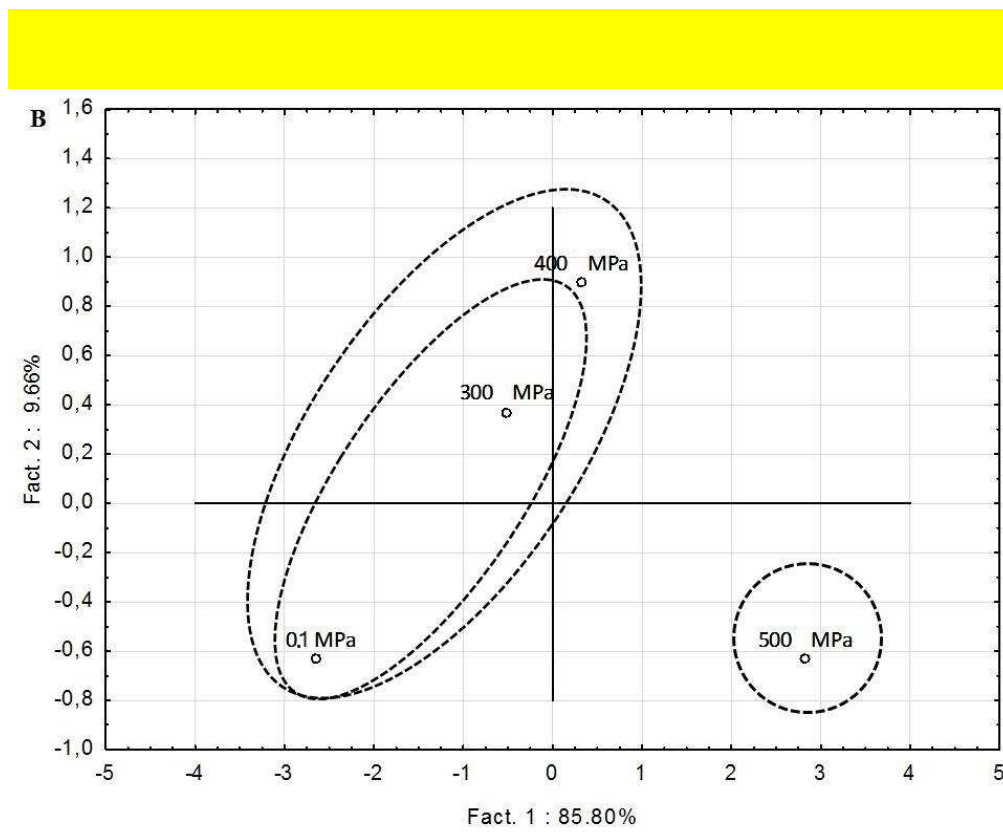
514

515

516 **Figure 4**



517



518 **Table 1: Spectral properties and contents of the main phycobiliproteins in *Porphyridium cruentum* (Fuentes, Fernández, Pérez, &**
 519 **Guerrero, 2000; Gantt & Lipschultz, 1974)**
 520

Name	Characteristic wavelengths of the main peak (nm) ^b	Shoulder(s) (nm) ^b	Characteristic lengths of the secondary peak (nm) ^b	wave	Average amount (mg 100g ⁻¹ dry weight) ^a	Proportion of all the phycobiliproteins (w/w) ^a
B-phycoerythrin (B-PE)	545 and 563	495-500	310		2020 ± 391	42
b-phycoerythrin (b-PE)	545	563	310			42
R-phycoerythrin (R-PE)	555 and 617	-	-		262 ± 70	11
Allophycocyanin (APC)	650	600 and 630	-		216 ± 54	5

521

522 ^a : data from (Fuentes *et al.*, 2000)

523 ^b : data from (Gantt & Lipschultz, 1974)

524 **Table 2: B-phycoerythrin content and its structure parameters in extracts obtained from *Porphyridium cruentum* as a function of the**
 525 **applied high hydrostatic pressure. Data is shown as mean (n = 3). Common letters indicate no significant difference between the values**
 526 **according to ANOVA (p < 0.05).**

HHP (MPa)	0.1	50	100	200	300	400	500
B-phycoerythrin (mg g ⁻¹ dry biomass)	66.1 ^a	66.7 ^a	65.5 ^a	66.5 ^a	65.5 ^a	62.8 ^{ab}	61.9 ^b
B-phycoerythrin fluorescence emission yield (.10 ⁵ (mg/g dry biomass) ⁻¹)	5.1 ^a	5.1 ^a	5.2 ^a	5.2 ^a	5.0 ^a	4.8 ^b	4.1 ^{5c}
Peak 2 enthalpy (J g ⁻¹ fresh sample)	0.0141 ^a	nd	nd	nd	0.0101 ^a	0.0099 ^a	0.0041 ^b

527 **Table 3: Correlation matrix based on PCA analysis.**

	Pressure	[B-PE]	B-PE Fluorescence Yield	Peak 1 Enthalpy	Peak 2 Enthalpy	Peak 3 Enthalpy
Pressure	1	- 0.88	- 0.82	- 0.98	- 0.91	0.69
[B-PE]	- 0.88	1	0.90	0.77	0.85	- 0.67
B-PE Fluorescence Yield	- 0.82	0.90	1	0.70	0.96	- 0.92
Peak 1 Enthalpy (J g ⁻¹)	- 0.98	0.77	0.70	1	0.84	- 0.61
Peak 2 Enthalpy (J g ⁻¹)	- 0.91	0.85	0.96	0.84	1	- 0.93
Peak 3 Enthalpy (J g ⁻¹)	0.69	- 0.67	- 0.92	- 0.61	- 0.93	1

528